

# The simple model to estimate the force exerted on the sphere rolling up a granular slope

Takeshi Fukumoto<sup>1,\*</sup>, Ken Yamamoto<sup>1</sup>, Makoto Katsura<sup>1</sup>, and Hiroaki Katsuragi<sup>1</sup>

<sup>1</sup>Department of Earth and Space Science, Osaka University, 1-1 Machikaneyama, Toyonaka, Osaka, 560-0043, Japan

**Abstract.** Spheres rolling on a granular bed sometimes experience a "stuck" phenomenon: translational motion ceases while rotational motion continues. To explore this phenomenon, we investigate the interaction between the granular slope and the sphere rolling up the slope using data obtained by Fukumoto et al. (PRE 109, 014903, 2024). Their experimental results confirmed the stuck phenomenon. According to these results, both translational and rolling motions exhibited constant deceleration until the translational motion halted. In this study, we propose a simple force model, following the approach proposed by Texier et al. (EPL 123, 54005, 2018). We estimate two forces acting on the sphere at a point slightly shifted from its bottommost point, both before and during the stuck phenomenon: one in the tangential direction and the other in the normal direction at a point on the surface of the sphere defined relative to an angle  $\theta_m$  from the axis perpendicular to the slope surface. Our analysis indicates that the normalized tangential and normal forces remain nearly constant for the slope angle and are independent of the density of the sphere, both before and during the stuck motion. Finally, by comparing the magnitudes of these forces and  $\theta_m$  before and during the stuck motion, we find that the point of force application shifts while the forces themselves remain nearly unchanged. This stuck phenomenon occurs when the translational force becomes insufficient owing to a change in  $\theta_m$ , even though the magnitudes of the forces remain unchanged.

## 1 Introduction

While driving on a loose sand surface, wheels sometimes become stuck. For example, in 2009, the Mars rover Spirit became stuck, ultimately ending its mission to explore the Martian environment [1]. Understanding the mechanism behind this stuck phenomenon is crucial for developing safer and more reliable vehicles for such challenging terrains.

To understand the interaction between soil and wheels, traditional terramechanics models have been developed to predict the forces exerted on a wheel by soil [2]. For example, in the model proposed in [2], the vertical stress distribution on a wheel rolling over deformable terrain was estimated using penetration tests, in which a flat plate was pushed into the sand. Shear stress was determined through flat plate shear tests to establish the relationship between normal and shear stresses. Traction and resistance forces were then calculated by integrating the stress over the contact area.

However, these terramechanics models require numerous fitting parameters (typically around 10), making the accurate estimation of soil parameters complex and time-consuming. Additionally, because these models focus on steady-state conditions (constant velocity or angular velocity of vehicle), they cannot account for transient phenomena, such as becoming stuck.

Our objective is to understand the stuck phenomenon using a simple model by introducing a basic experimental system to examine its fundamental aspects. To investigate the primary interaction between an object and soil, we focus on the dynamics of a sphere rolling on a granular surface. Previous studies explored the dynamics of a sphere rolling down [3, 4] or rolling up [5] a granular slope, as well as rolling on a horizontal granular surface [6]. These experiments revealed that the dynamics of the sphere follow constant deceleration [3, 5, 6] or acceleration [4].

Only Fukumoto et al. quantitatively investigated the stuck phenomenon, observing that the rolling motion ceases after the translational motion halts [5]. They characterized the dynamics of the sphere by simultaneously measuring its translational and rolling motions and analyzing energy dissipation. However, their analysis focused only on the motion prior to the stuck event. As a result, the dynamics involved in the stuck motion itself were not analyzed, leaving their analysis insufficient for a complete understanding of the stuck phenomenon.

To analyze the stuck motion, we estimate the instantaneous forces acting on the sphere from the granular slope using the data obtained in [5]. We employ the force model developed by [4], which assumes that two forces—tangential and normal—are exerted at a single point on the sphere as it rolls down a granular slope. By applying this model to the data from [5], we compute the point of force application and the instantaneous forces in both the tangential and normal directions for the sphere

\*e-mail: t.fukumoto@ess.sci.osaka-u.ac.jp

rolling up a granular slope. Finally, we compare these values (two forces and points) before and during stuck motion.

## 2 Material and methods

To measure the dynamics of the sphere, we use the experimental data from [5] shown in Fig. 1 (a). In this setup, a sphere rolls up an inclined bed of glass beads with a typical diameter of 0.8 mm. The spheres used in this experiment are made of polyethylene, polyacetal, glass, or alumina ceramic, all with a radius  $R = 6.35$  mm. Their densities are  $\rho_s = 930, 1400, 2600,$  and  $3900$  kg/m<sup>3</sup>, respectively. The dynamics of the sphere rolling up a granular slope are investigated with varying initial velocity  $v_0$  (the velocity when the sphere enters the granular surface) ranging from 0.2 to 0.7 m/s. The slope angle  $\alpha$  is varied from  $\alpha \approx 0^\circ$  to  $20^\circ$ . We measure the position of the center of the sphere and its rolling posture. We define  $L$  as the maximum distance reached in the  $X$  direction and  $\delta$  as the sinking depth along the gravity direction. For further details on the experimental setup, please refer to our previous report [5].

## 3 Results

In Figs. 2 (a) and (b), typical examples of the translational velocity  $v_X(t)$  and angular velocity  $\omega(t)$  are shown, respectively. Here,  $t$  represents the elapsed time from the moment the sphere enters the granular surface. Note that both quantities,  $v_X(t)$  and  $\omega(t)$ , linearly decrease over time, indicating that the dynamics of the sphere on the granular slope exhibit constant deceleration. By fitting the data to a linear function from  $t = 0$  to  $t = t_{\text{stop}}$  ( $t_{\text{stop}}$  is defined by  $v_X(t_{\text{stop}}) = 0$ ), the slopes of the fitting lines,  $a_X$  (translational deceleration) and  $\dot{\omega}$  (angular deceleration), can be obtained from the experimental results. As shown in Fig. 2 (b), the condition  $\omega(t_{\text{stop}}) > 0$  indicates that the translational and rolling motions do not halt simultaneously. This situation is defined as stuck motion. During the stuck motion, from  $t = t_{\text{stop}}$  to the time at which  $\omega = 0$  is reached, we assume that the angular deceleration  $\dot{\omega}$  remains constant in both  $t < t_{\text{stop}}$  and  $t > t_{\text{stop}}$ , as represented the black line in Fig. 2 (b).

## 4 Analysis and Discussion

We propose a model to estimate the force exerted on a sphere rolling up a slope as shown in Fig. 1 (b), similar to the model reported in [4]. We assume two forces:  $F_R$  (normal force) and  $F_\theta$  (tangential force), which act at a point where the force balance in the direction normal to the slope is satisfied. We define  $\theta_m$  as the slope of the surface of the sphere relative to the axis perpendicular to the surface, where  $F_R$  and  $F_\theta$  are acting. As shown in Fig. 2, the sphere rolls up with constant translational acceleration  $a_X$  and angular acceleration  $\dot{\omega}$ . In this situation, the values of  $F_R$ ,  $F_\theta$ , and  $\theta_m$  are calculated as described below.

According to the rolling equation of motion, the force in the rolling direction is expressed as

$$I\dot{\omega} = -RF_\theta, \quad (1)$$

where  $I = 2MR^2/5$  ( $M$  is the mass of the sphere) is the moment of inertia of the homogeneous sphere.

By assuming the force balance in the  $Y$  direction (perpendicular to the slope surface),  $F_R$  and  $F_\theta$  obey the relation

$$Mg \cos \alpha = F_R \cos \theta_m + F_\theta \sin \theta_m, \quad (2)$$

where  $g$  is the magnitude of gravitational acceleration.

By considering the translational equation of motion along the  $X$  direction (along the slope surface), we can obtain the relation

$$Ma_X = F_\theta \cos \theta_m - F_R \sin \theta_m - Mg \sin \alpha. \quad (3)$$

Combining Eqs. (1), (2), and (3), we can calculate the values of  $F_R$ ,  $F_\theta$ , and  $\theta_m$  using  $a_X$  and  $\dot{\omega}$ , which can be experimentally measured.

The calculated  $F_R/Mg$  and  $F_\theta/Mg$  are shown in Fig. 3 (a). As seen in Fig. 3 (a),  $F_R/Mg$  and  $F_\theta/Mg$  are almost independent of  $\alpha$  or  $\rho_s$ . Thus, we can assume that they are constant values:  $F_R/Mg = 0.96 \pm 0.04$  and  $F_\theta/Mg = 0.26 \pm 0.04$ . The calculated  $\theta_m$  is shown in Fig. 3 (b). Note that  $\theta_m$  increases with  $\rho_s$ . It remains almost constant for  $\alpha < 0.3$  rad and decreases for  $\alpha > 0.3$  rad. However, the value of  $\theta_m$  for the polyethylene sphere remains constant with respect to  $\alpha$ . In this study, we assume that the force balance in the  $Y$  direction is always satisfied [Eq. (2)]. However, this condition may not hold for  $\alpha > 0.3$ , especially in the high  $\rho_s$  regime. **As  $\alpha$  increases,  $L$  decreases due to the greater influence of gravity. With increasing  $\rho_s$ ,  $\delta$  increases [5], and the motion can no longer be approximated as purely in the  $X$  direction.**

Note also that  $\theta_m$  increases with  $\rho_s$  as  $\delta$  also increases with  $\rho_s$  [5]. Next, we examine the relationship between  $\theta_m$  and  $\delta$ . To this end, we introduce the angle  $\theta_f$  to characterize the contact zone with the glass beads. This angle satisfies  $\cos \theta_f = 1 - \frac{\delta}{R}$ . The relation between  $\theta_m$  (for data with  $\alpha < 0.3$ ) and  $\theta_f$  is shown in Fig. 4. By fitting the data to a squared relation, we obtain the expression  $\theta_m = 0.28 + 0.12\theta_f^2$  [Fig. 4]. Note that  $\theta_m$ , which is related to the resistance force of the sphere, is determined by  $\delta$  (and its function  $\theta_f$ ). The detailed origin of this curve is discussed in APPENDIX. **This curve differs from that of Texier et al. [4] in functional form and intercept, likely due to the difference between rolling up and down the slope.**

Then, we calculate the values of  $F_R$ ,  $F_\theta$ , and  $\theta_m$  after  $t_{\text{stop}}$  ( $v_X = 0$  and  $\omega > 0$ ). We assume that  $\dot{\omega}$  ( $t \geq t_{\text{stop}}$ ) is the same as  $\dot{\omega}$  ( $t < t_{\text{stop}}$ ), as shown in Fig. 2 (b). By considering  $a_X = 0$  and substituting  $\dot{\omega}$  obtained from Fig. 2 (b) into Eq. (1),  $F_R$ ,  $F_\theta$ , and  $\theta_m$  are calculated. As shown in Fig. 5 (a),  $F_R/Mg$  and  $F_\theta/Mg$  are almost independent of  $\alpha$  or  $\rho_s$ . Thus, we can assume they are constant values:  $F_R/Mg = 0.96 \pm 0.01$  and  $F_\theta/Mg = 0.26 \pm 0.04$ . These values coincide with those before the stuck motion. Note that seen in Fig. 5 (b),  $\theta_m$  shows a decreasing tendency with  $\alpha$  and is almost independent of the density of the sphere  $\rho_s$ . By fitting a line with a slope of  $-1$ , we obtain the relation  $\theta_m = 0.26 - \alpha$  represented by the solid line in Fig. 5 (b). The sum  $\theta_m + \alpha$  represents the angle seen from the gravity direction; this angle can be considered as constant with a

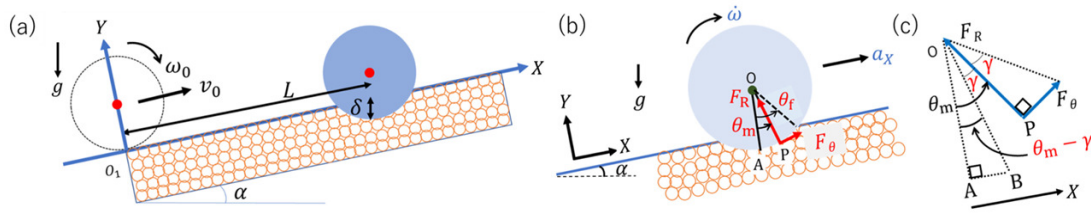


**Figure 1.** (a) Schematic image of the experimental setup. By varying the initial velocity  $v_0 = 0.2 - 0.7$  m/s (and  $\omega_0$ ) and slope angle  $\alpha = 0^\circ - 20^\circ$ , we measure the maximum translational migration length  $L$ , vertical sinking depth  $\delta$ , and both translational and rolling decelerations. The  $X$  axis is along the granular surface whereas the  $Y$  direction is perpendicular to the slope. (b) Notations used in the model. When the sphere rolls up the granular slope with acceleration  $a_X$  and angular acceleration  $\dot{\omega}$ , the sphere experiences two forces,  $F_R$  (normal force) and  $F_\theta$  (tangential force), at the contact point at the angle of  $\theta_m (= \angle AOP)$  in (c);  $\theta_f$  is the contact angle from the  $Y$  direction. (c) A partially magnified view of the panel (b). The angle  $\gamma$  is defined as  $\gamma = \arctan(F_\theta/F_R)$ . Point B must be positioned such that  $OA \perp AB$  and  $\angle POB = \gamma$ .

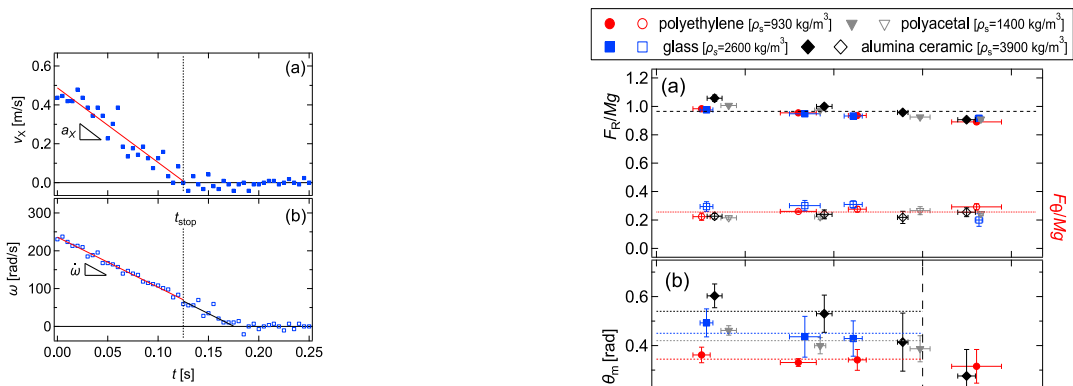


**Figure 2.** (a) Translational velocity  $v_X$  as a function of time  $t$  at  $\alpha \approx 15^\circ$  for a glass sphere. By performing a least-square fit to the linear function from  $t = 0$  to the stopping time  $t_{\text{stop}}$  (where  $v_X(t_{\text{stop}}) = 0$ ), a nearly constant deceleration  $a_X$  can be obtained. (b) Angular velocity  $\omega$  as a function of time  $t$  at  $\alpha \approx 15^\circ$  for a glass sphere. Similarly, by least-square fitting to a linear function (from  $t = 0$  to  $t_{\text{stop}}$ ), a nearly constant deceleration  $\dot{\omega}$  can be obtained. The black straight line extends this deceleration slope  $\dot{\omega}$  from  $t = t_{\text{stop}}$  till  $\omega = 0$ , assuming the same deceleration rate during the stuck phase.

**Figure 3.** (a) Relations between  $F_R/Mg$  (filled symbols),  $F_\theta/Mg$  (empty symbols) and  $\alpha$ . The dashed and dotted lines represent the averages,  $F_R/Mg = 0.96 \pm 0.04$  and  $F_\theta/Mg = 0.26 \pm 0.04$ , respectively. (b) Relation between  $\theta_m$  and  $\alpha$ . The dotted lines indicate the average of  $\theta_m$  in the range of  $\alpha < 0.3$  for each  $\rho_s$ . Error bars in both (a) and (b) indicate the standard deviation of the data for various  $v_0$  cases.

value of 0.26 rad during the stuck motion. The reason for this constancy is under consideration.

We discuss the mechanism of the stuck phenomenon by comparing the values of  $F_\theta$ ,  $F_R$ , and  $\theta_m$  before  $t_{\text{stop}}$  and during stuck motion. The values of  $F_R/Mg$  and  $F_\theta/Mg$  are constants, independent of experimental conditions and slipping situations. It can be assumed that the position where the forces  $F_\theta$  and  $F_R$  are applied changes. However, the reason why the angle at which the forces are applied changes is still under investigation.

## 5 Conclusions

We experimentally investigate a sphere rolling up a granular slope to estimate the force acting on it. Given that the translational and rolling dynamics of the sphere exhibit constant deceleration, we use a model to estimate the constant forces in both the normal and tangential di-

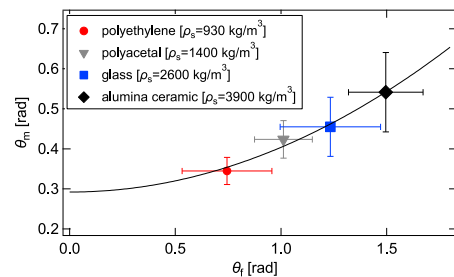


**Figure 4.** Relation between  $\theta_m$  and  $\theta_f$  from the data for  $\alpha < 0.3$ . Error bars indicate the standard deviation for various  $v_0$  cases (in the range of  $\alpha < 0.3$ ). The solid curve represents fitting to a parabolic function. We obtain a relation between  $\theta_m$  and  $\theta_f$  expressed as  $\theta_m = 0.28 + 0.12\theta_f^2$ .

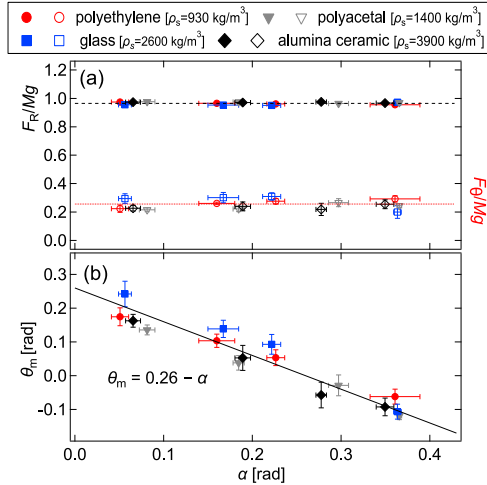


**Figure 5.** (a) Relations between  $F_R/Mg$  (filled symbols),  $F_\theta/Mg$  (empty symbols) and  $\alpha$  during the stuck motion. The dashed and dotted lines represent the averages,  $F_R/Mg = 0.96 \pm 0.01$  and  $F_\theta/Mg = 0.26 \pm 0.04$ , respectively. (b) Relation between  $\theta_m$  and  $\alpha$  during the stuck motion. The solid line indicates a fitting line with a slope of  $-1$ ,  $\theta_m = 0.26 - \alpha$ . Error bars in both (a) and (b) indicate the standard deviation of the data for various  $v_0$  cases.

rections. We introduce two forces (tangential  $F_\theta$  and normal  $F_R$ ) and the angle  $\theta_m$ . From the experimental results, the constant normalized forces are obtained as  $F_R/Mg = 0.96 \pm 0.04$  and  $F_\theta/Mg = 0.26 \pm 0.04$ . The angle  $\theta_m$  remains nearly constant for  $\alpha < 0.3$  rad, and  $\theta_m$  and  $\theta_f$  follow a quadratic relation. The angle  $\theta_f$  represents the contact area when the sphere sinks by  $\delta$ . This suggests that  $\theta_m$ , which is correlated with the resistance force, is related to  $\delta$ .

Based on the experimental observations, we conclude that  $\dot{\omega}$  ( $t > t_{\text{stop}}$ ) during the stuck motion remains the same as before becoming stuck,  $\dot{\omega}$  ( $t < t_{\text{stop}}$ ). According to this assumption,  $F_\theta$ ,  $F_R$ , and  $\theta_m$  are computed. The constant normalized forces obtained are  $F_R/Mg = 0.96 \pm 0.01$  and  $F_\theta/Mg = 0.26 \pm 0.04$ . They are identical to those before the sphere becomes stuck. We also observe that  $\theta_m$  decreases with  $\alpha$  and  $\theta_m$  remains nearly independent of  $\rho_s$ . By applying linear fitting, we find the relation  $\theta_m = 0.26 - \alpha$ . This suggests that the angle where the forces are applied relative to the gravity direction remains constant at 0.26 rad during the stuck motion. The universality of this value should be investigated in future studies.

By comparing the values of  $F_\theta$ ,  $F_R$ , and  $\theta_m$  at  $t < t_{\text{stop}}$  and  $t > t_{\text{stop}}$ , we analyze the mechanism of the stuck phenomenon. We find that the magnitudes of the forces  $F_\theta$  and  $F_R$  remain unchanged, but the angle at which these forces are applied changes. Consequently, the force required for forward motion is no longer generated.

## ACKNOWLEDGMENTS

This study was supported by JST SPRING No. JP-MJSP2138 and JSPS KAKENHI No. JP24H00196.

## APPENDIX

We derive the relation between  $\theta_m$  and  $\theta_f$  by comparing the current model with that of [5]. To estimate the normalized energy dissipation in translational direction, they considered the energy balance in translational motion [5]. Accordingly,  $\mu_d$  (an effective friction coefficient) can be expressed as

$$\mu_d = -\frac{a_x/g + \sin \alpha}{\cos \alpha} + \frac{\delta}{L \cos \alpha}. \quad (4)$$

By combining Eqs. (2), (3), and (4), we obtain the relation,

$$\mu_d - \frac{\delta}{L \cos \alpha} = \tan(\theta_m - \gamma). \quad (5)$$

Here,  $\gamma$  satisfies  $\gamma = \arctan(F_\theta/F_R)$ , as shown in Fig. 1 (c). Note that  $\frac{\delta}{L \cos \alpha}$  is the intrusion angle. Given that  $\tan(\theta_m - \gamma) \approx \theta_m - \gamma$  (for  $\theta_m - \gamma \approx 0$ ), the right side of Eq. (5) can be approximated as  $\theta_m - \gamma$ . In [5], the relationship  $\mu_d \propto \delta/R$  is confirmed. By assuming that the term  $\frac{\delta}{L \cos \alpha}$  can be neglected, the left side of Eq. (5) becomes proportional to  $\delta/R$ . Given that  $\cos \theta_f \approx 1 - \frac{\theta_f^2}{2}$  (for  $\theta_f \approx 0$ ), it follows that  $\delta/R \propto \theta_f^2$ . Thus, we obtain the relation,  $\theta_m - \gamma \propto \theta_f^2$ .

## References

- [1] K. Sanderson, Mars rover Spirit (2003–10). *Nature* **463**, 600 (2010). <https://doi.org/10.1038/463600a>
- [2] J.-Y. Wong and A.R. Reece, Prediction of rigid wheel performance based on the analysis of soil-wheel stresses part I. Performance of driven rigid wheels. *Journal of Terramechanics* **4**, 81 (1967). [https://doi.org/10.1016/0022-4898\(67\)90105-X](https://doi.org/10.1016/0022-4898(67)90105-X)
- [3] F. V. De Blasio and M.-B. Saeter, Rolling friction on a granular medium. *Physical Review E* **79**, 022301 (2009). <https://doi.org/10.1103/PhysRevE.79.022301>
- [4] B. D. Texier, A. Ibarra, F. Vivanco, J. Bico, and F. Melo, Friction of a sphere rolling down a granular slope. *Europhysics Letters* **123**, 54005 (2018). <https://dx.doi.org/10.1209/0295-5075/123/54005>
- [5] T. Fukumoto, K. Yamamoto, M. Katsura, and H. Katsuragi, Energy dissipation of a sphere rolling up a granular slope: Slip and deformation of the granular surface. *Physical Review E* **109**, 014903 (2024). <https://doi.org/10.1103/PhysRevE.109.014903>
- [6] S. V. Wal, S. Tardivel, P. Sánchez, D. Djafari-Rouhani, and D. Scheeres, Rolling resistance of a spherical pod on a granular bed. *Granular Matter* **19**, 17 (2017). <https://doi.org/10.1007/s10035-016-0696-z>